Stochastic Desertification

Haim Weissmann and Nadav M. Shnerb
Department of Physics, Bar-Ilan University, Ramat-Gan IL52900, Israel

The process of desertification is usually modeled as a first order transition, where a change of an external parameter (e.g. precipitation) leads to a catastrophic bifurcation followed by an ecological regime shift. However, vegetation elements like shrubs and trees undergo a stochastic birth-death process with an absorbing state; such a process supports a second order continuous transition with no hysteresis. We present a numerical study of a minimal model that supports bistability and catastrophic shift on spatial domain with demographic noise and an absorbing state. When the external parameter varies adiabatically the transition is continuous and the front velocity renormalizes to zero at the extinction transition. Below the transition one may identify three modes of desertification: accumulation of local catastrophes, desert invasion and global collapse. A catastrophic regime shift occurs as a dynamical hysteresis, when the pace of environmental variations is too fast. We present some empirical evidence, suggesting that the mid-holocene desertification of the Sahara was, indeed, continuous.

PACS numbers: 87.10.Mn,87.23.Cc,64.60.Ht,05.40.Ca

arXiv:1401.0160v1 [q-bio.PE] 31 Dec 2013

The catastrophic bifurcation and its statistical mechanics analog, the first order transition, play a central role in the physical sciences. In these processes a tiny change in the value of an external parameter leads to a sudden jump of the system from one phase to another. This change is irreversible and is accompanied by hysteresis: once the system relaxed to its new phase, it will not recover even when the external parameters are restored.

The relevance of these processes to the ecology of population and communities has been established while ago [1]. Recently, there is a growing concern about the possible occurrence of regime shifts in ecological systems [2–5]. The anthropogenic changes of local and global environmental parameters from habitat fragmentation to the increasing levels of CO2 in the atmosphere - raise anxiety about the possibility of an abrupt and irreversible catastrophe that may be destructive to the functions and the stability of an ecosystem [6]. This concern triggered an intensive search for empirical evidence that may allow one to identify an impending tipping point, where the most popular suggestion is to use the phenomenon of critical slowing down [5, 7–11]. Other suggested early warning indicators, especially for sessile species, deal with spatial patterns and the level of aggregation [4, 12, 13]

Of particular importance is the process of desertification, which is considered as an irreversible shift from the "active" vegetation state to the "inactive" bare soil state, resulting from an increased pressure (e.g., overgrazing, declines in precipitation). As drylands cover about 41% of Earth land surface, desertification affects about 250 million people around the world [14]. Various models show that, when the vegetation state has a *positive feedback*, like an increased runoff interception or reduced evaporation close to vegetation patches, the system supports two attractive fixed points (alternate steady states) [13, 15]. The bare soil fixed point is stable, since the desert is robust against small perturbation (a small amount of vegetation) for which the positive feedback is too weak while the active state is self-sustained. Accordingly, the system may cross over from vegetation to bare soil in two routes: First, a disturbance that pushes the system to the basin of attraction of the bare soil fixed point, and second, when the vegetation fixed point losses stability, i.e., when a change of an external parameter takes the system over its tipping point [16].

However, the bare soil is an *absorbing state*: it corresponds to a complete destruction of the vegetation (or at least of a given species), hence it is not affected by noise. In a finite system the process must reach eventually the absorbing state. In the thermodynamic limit the steady state solution depends on the ratio between the rate of local extinction and the chance of recolonization from neighboring sites. This dynamics resembles the contact (SIS) process [17, 18] where the extinction transition is continuous and belongs to the directed percolation (DP) universality class. Accordingly, one should expect a *reversible* second order desertification, with no jumps, no hysteresis and no tipping point.

Here we present a study of a minimal model for desertification with demographic noise. When the external parameter sweep is adiabatic the transition is indeed DP continuous, as [19] have already pointed out. We analyze numerically the system beyond the extinction transition point, showing that it admits different modes of desertification in different areas of the parameter space. We identify these modes, consider the effect of the absorbing state on the velocity of the front, and discuss (qualitatively) the conditions under which the deterministic first order transition scenario is a reasonable approximation.

The model used below is a simple version of the Ginzburg-Landau (GL) equation where the biomass den-

sity b vanishes at one of the fixed points,

$$\frac{\partial b}{\partial t} = D\nabla^2 b - \alpha b + \beta b^2 - \gamma b^3. \quad (1)$$

Here D is the diffusion constant, The control parameter α represent the effect of the (changing) environment, β is a positive constant that represents local facilitation, and the positive constant γ accounts for the finite carrying capacity of the system. When the environment is hostile [positive value of "stress parameter" α, in Eq. (1)] the absorbing (desert) state $b = 0$ is locally stable but local facilitation may allow the system to have another stable state at a finite vegetation density. Negative values of α correspond to better environmental conditions, where the absorbing state is unstable (See the bifurcation diagram (lines) in Figure 1).

The deterministic equation (1) admits one or two homogenous solutions, depending on the value of α. Catastrophic desertification occurs beyond the tipping point, i.e., when $\alpha \geq \beta^2/(4\gamma)$, where the system collapses to its desert state following a saddle-node bifurcation. To recover vegetation, the stress parameter α should cross zero (transcritical bifurcation), so the regime shift is irreversible.

When the initial conditions are inhomogeneous, the desert invades the vegetation to the right of the Maxwell (melting) point $\alpha_m > 2\beta^2/(9\gamma)$, and vegetation invades on its left side (see Fig. 1) . The importance of the Maxwell point was emphasized recently by Bel et. al. [20] (see also Durrett and Levin [21]): once the system crosses the Maxwell point, any large disturbance that will generate a large-enough bare-soil region will invade the rest of the system and lead to desertification.

Stochasticity in an ecosystem occurs even when rates of demographic processes (birth, death, migration etc.) are independent of time, reflecting the randomness of the birth/death process at the individual level [4, 12, 22]. For example, if B represent a unit of biomass (a shrub, say), the quadratic term of Eq 1 may emerge as the deterministic limit of the process $B + B \xrightarrow{\beta} 3B$, the cubic term emerges from $B + B + B \xrightarrow{\gamma} \oslash$ and the linear term corresponds to $B \xrightarrow{\alpha} \oslash$ (if $\alpha \geq 0$) or $B \xrightarrow{\alpha} 2B$ if $\alpha \geq 0$. *Demographic stochasticity* of this kind yields, for a population of size N, fluctuations amplitude that scale with $\sqrt{N}$. As mentioned above, in a single site or a finite domain the system eventually reach the absorbing state at $b = 0$, although the timescale for this process may be large [23, 24]. For a spatial system, with migration of individuals to neighboring sites in a rate proportional to D, the system undergoes an extinction transition when the rate of recolonization of empty sites is equal to the rate of local extinctions [17].

Eq. (1) appears to be the deterministic limit of this stochastic process, obtained when N, the number of particles per site (the model is defined off lattice, but any discretization procedure should involve, at least indirectly, a UV cutoff defined by the "size" of an individual, or the interaction range), goes to infinity. This convergence of a stochastic process to the corresponding PDE's was analyzed in [18, 25], and was shown to fail close to the extinction transition, when fluctuations govern the dynamics even in the large N limit. This failure is limited to a narrow region close to the transition point, and the width of the transition zone approaches zero like $N^{-\kappa}$, where the exponent $\kappa = 2/(d_c - d)$ depends on the upper critical dimension of the transition and on the dimensionality of the system. The analysis of [18, 25] takes into account two prototypes of out-of-equilibrium phase transitions, the SIS process [26] that belongs to the directed percolation universality class and the SIR process [27] that belongs to the dynamic percolation universality class. However, these two transitions are continuous even in the deterministic limit, while our system admits a first-order transition when $N \to \infty$

Kockelkoren and Chaté [19] have already discussed this issue, showing that the extinction transition is indeed second order (DP) once the absorbing state is taken into account. This result is demonstrated in Figure 1. Our simulation technique is close to the split-step method used by [19, 28, 29]: an Euler integration of Eq. 1 (with $\Delta t = 0.001$, $1d$ lattice of $L = 10000$ sites, asynchronous update) is interrupted every ζ generations when the value of b_i at every site i is replaced by an integer, taken from a Poisson distribution with an average b_i. We have verified that the transition has, indeed, the critical exponent of the directed percolation equivalence class [17].

In Fig 1 the equilibrium density is plotted as a function of α for different values of ζ and D, together with the deterministic bifurcation diagram. The stochastic transition is indeed continuous, but one observes a new feature: even close to the deterministic limit (large values of ζ or D) the transition point cannot cross the Maxwell line. As long as ζ and D are finite, local extinctions happen with nonzero probability [23], and once a local "hole" is opened, it will spread and overtake the vegetation if the system is above the Maxwell point [20]. This implies that the failure of the system to converge to its deterministic behavior in the $N \to \infty$ limit is not limited to a single point (like in the SIS/SIR cases) but to a finite domain between the Maxwell point and the tipping point.

Figure 1 also indicates that, when the noise is relatively weak, the vegetation steady state density decays *linearly* as the system approaches the extinction transition. The DP theory predicts a steady state density that scales like $\Delta^{\tilde{\beta}}$, where Δ is the distance from the transition and $\tilde{\beta} < 1$ below d_c. This is indeed the case very close to the transition point (result not shown here) but here the system should converge to the deterministic limit at large Δ, so the transition region is very narrow and the growth appears to be linear.

The hypothesis of a second-order, reversible desertification transition with a linear decay of the steady-state

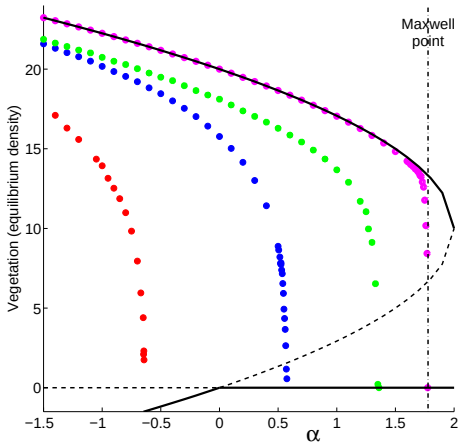

FIG. 1: **The desertification transition**. The lines represent the possible steady states of the spatially homogenous solution of Eq. (1) with $\beta = 0.4, \gamma = 0.02$. Full lines correspond to stable fixed points, dashed lines to unstable points. The transcritical bifurcation at $\alpha = 0$ and the saddle-node bifurcation (tipping point) at $\alpha = 2$ are clearly seen. The Dash-dot line indicates the Maxwell point. The symbols are the steady state density obtained from numerical solutions of the process with different αs for $D = 0.2, \zeta = 30$ (red), $D = 0.2, \zeta = 60$ (blue), $D = 10, \zeta = 30$ (green), $D = 0.2, \zeta = 3000$ (purple). The transition point cannot cross the Maxwell point.

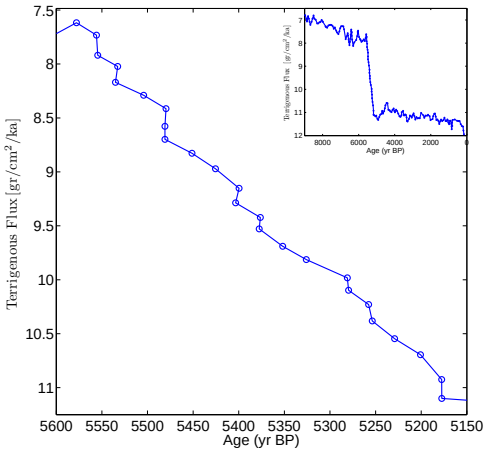

FIG. 2: The mid-Holocene desertification of the Sahara, as expressed by the increase of the flux of terrigenous dust, during the last 9000 years (inset) and during the transition period (main panel, modified from [35]). The transition is assumed to be triggered by a gradual and weak decline of the Northern Hemisphere summer insolation [2, 35].

density in the transition regime, is supported by two pieces of data. Reversibility is suggested by a few recent studies, showing a recovery from desertification when the external pressure (grazing, in most cases) has been removed [30–34]. Some evidence for linearity are suggested in Figure 2, where the desertification process of the Sahara during the mid-Holocene is traced through the eolian dust record of Site 658C [35]. The flux of terrigenous sediments seem to grow linearly during the transition period, in agreement with the predictions of our model.

Note that the Sahara desertification data are usually interpreted (see, e.g., [2]) as an evidence for a catastrophic, first order transition, since the growth of terrigenous sediments *percentage* through time appears to be exponential. However, as stressed in [36], the use of component percentages in marine sediments can be misleading, because the total sediment must always sum to 100%. The long timescales involved (about 500 years) also suggest an alternative mechanism.

By studying the system with inhomogeneous initial conditions and monitoring the growth of the overall density vs. time we have measured the front velocity v. In the deterministic limit the velocity satisfies,

$$v = \pm\sqrt{2D}\left(\frac{-\alpha}{m} + \frac{m}{2}\right) \tag{2}$$

where

$$m \equiv \sqrt{-\alpha + \frac{\beta^2}{\gamma}\left(\frac{1}{2} + \sqrt{\frac{1}{4} - \frac{\gamma\alpha}{\beta^2}}\right)}. \tag{3}$$

The velocity changes sign in the Maxwell point, where the front changes its characteristic, from a Ginzburg-Landau front to Fisher type II, at the transcritical bifurcation [37, 38]. However, as shown in Figure 3, under demographic stochasticity the velocity renormalizes to zero at the extinction transition point.

The emerging insights are summarized in Fig 4. For every set of parameters (diffusion, noise, nonlinear interaction) the system admits four different phases. Above the extinction transition (region 1) vegetation saturates to an equilibrium value and will invade a nearby bare-soil region. The steady state density and the front velocity both vanishes in all other regions, but desertification takes place in different modes. In region 2 (between the extinction point and the Maxwell point) the desert does not invade, and the transition comes about by accumulation of local extinctions eventuating a global collapse. In region 3 these collapses are accompanied by the desert invasion predicted by [20] and the dominant effect depends on the size of the system and the velocity of the front. Finally, beyond the tipping point (Region 4) the deterministic active fixed point loses its stability and vegetation collapse exponentially, simultaneously all over the place.

All in all, for every system that admits an absorbing state, if environmental changes (like the rate of variations of α) are adiabatic, the phase transition is a continuous, second order one, without hysteresis. The catastrophe scenario - a global collapse after the crossing of the tip-

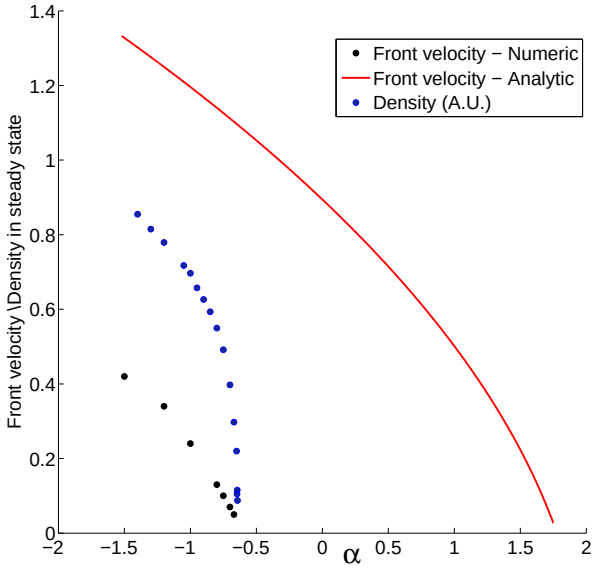

FIG. 3: **Invasion velocity renormalization.** Front velocity is shown against α. Blue circles represent the steady state density of the stochastic simulation for the same value of α (in arbitrary units). The black dots represent the front velocity measured in the simulation. Parameters are $\beta = 0.4, \gamma = 0.02, dt = 0.01, D = 0.2, \zeta = 30$. Given the numerical inaccuracies close to the transition, these two sets of circles seem to reach zero at the same point. The red line correspond to the analytic expression 2. (for these parameters $\alpha_{MP} = 1.778$). Front velocity was measured by monitoring the linear growth rate of the b density. The initial conditions are vegetation for $5000 < x < 10000$ and bare soil for $1 < x < 5000$.

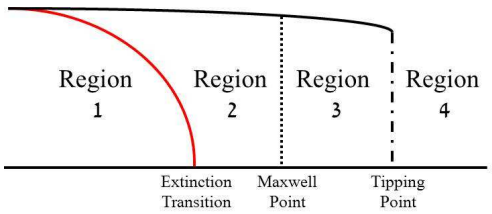

FIG. 4: **Modes of desertification - a schematic .** The steady-state density of vegetation (red line) approaches zero at the extinction transition. Between this point and the Maxwell point (region 2) the desertification happens in a series of local collapses. In region 3 there is also desert invasion, while in region 4 the collapse is global.

ping point, followed by an irreversible transition between alternative stable state, can never be realized. As long as ζ is finite, the transition is second order and, even more importantly, it cannot take place beyond the Maxwell point, so the tipping point is completely disparate from the extinction transition. Accordingly, the attempts to identify an impending catastrophe by analyzing fluctuation dynamics, utilizing the critical slowing down as an early warning signal, appears to be useless.

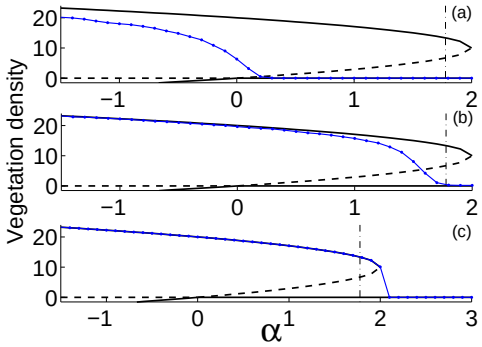

FIG. 5: **Dynamical hysteresis**: Vegetation density (blue) vs. α, depicted with the deterministic bifurcation diagram as a background (black), for $\alpha = -1.5 + s \cdot t$, $s = 10^{-5}$, with $\zeta = 40$ (a) 200 (b) and 1000 (c).

The studies of catastrophic shifts and early warning signals may be relevant to the desertification problem only if the environmental change is non-adiabatic, where the irreversibility has to be interpreted as a dynamical hysteresis [39]. This behavior is demonstrated in Figure 5. Dynamical hysteresis is unavoidable close to the extinction transition when the response of the system becomes slower than the pace of environmental change, but its effect may be very weak.

As each of the regions 1-4 (in Fig. 4) has its own characteristic timescale, the conditions for a "rapid" sweep rate are different in different regions. The deterministic picture is relevant only when the sweep rate for α is faster than any other process in the system. However, in such a case the implementation of critical slowing down indicators close to the tipping point, assuming that one can trace the relaxation of fluctuations before the catastrophic shift, may also become inefficient.

acknowledgments We would like to thank Baruch Meerson, Yoram Louzoun, Hila Behar, David Kessler and Ehud Meron for helpful discussions and useful comments. This work was supported by the Israeli Ministry of science TASHTIOT program and by the Israeli Science Foundation BIKURA grant no. 1026/11.

[1] R. M. May, Nature **269**, 471 (1977).
[2] M. Scheffer, S. Carpenter, J. A. Foley, C. Folke, and B. Walker, Nature **413**, 591 (2001).
[3] M. Rietkerk, S. C. Dekker, P. C. de Ruiter, and J. van de Koppel, Science **305**, 1926 (2004).
[4] S. Kéfi, M. Rietkerk, C. L. Alados, Y. Pueyo, V. P. Papanastasis, A. ElAich, and P. C. De Ruiter, Nature **449**, 213 (2007).
[5] M. Scheffer, J. Bascompte, W. A. Brock, V. Brovkin, S. R. Carpenter, V. Dakos, H. Held, E. H. Van Nes, M. Rietkerk, and G. Sugihara, Nature **461**, 53 (2009).

[6] A. K. Duraiappah, S. Naeem, T. Agardy, and M. E. Assessment, *Ecosystems and human well-being: biodiversity synthesis* (Island Press Washington DC, 2005).

[7] V. Dakos, M. Scheffer, E. H. van Nes, V. Brovkin, V. Petoukhov, and H. Held, Proceedings of the National Academy of Sciences **105**, 14308 (2008).

[8] C. Boettiger and A. Hastings, Proceedings of the Royal Society B: Biological Sciences **279**, 4734 (2012).

[9] T. M. Lenton, Nature Climate Change **1**, 201 (2011).

[10] L. Dai, D. Vorselen, K. S. Korolev, and J. Gore, Science **336**, 1175 (2012).

[11] L. Dai, K. S. Korolev, and J. Gore, Nature **496**, 355 (2013).

[12] T. M. Scanlon, K. K. Caylor, S. A. Levin, and I. Rodriguez-Iturbe, Nature **449**, 209 (2007).

[13] R. Solé, Nature **449**, 151 (2007).

[14] J. F. Reynolds, D. M. S. Smith, E. F. Lambin, B. Turner, M. Mortimore, S. P. Batterbury, T. E. Downing, H. Dowlatabadi, R. J. Fernández, J. E. Herrick, et al., science **316**, 847 (2007).

[15] K. N. Suding, K. L. Gross, and G. R. Houseman, Trends in Ecology & Evolution **19**, 46 (2004).

[16] M. Rietkerk, P. Ketner, L. Stroosnijder, and H. H. Prins, Journal of Range Management pp. 512–519 (1996).

[17] H. Hinrichsen, Advances in physics **49**, 815 (2000).

[18] D. A. Kessler and N. M. Shnerb, Physical Review E **85**, 051138 (2012).

[19] J. Kockelkoren and H. Chaté, arXiv preprint cond-mat/0208497 (2002).

[20] G. Bel, A. Hagberg, and E. Meron, Theoretical Ecology **5**, 591 (2012).

[21] R. Durrett and S. Levin, Theoretical population biology **46**, 363 (1994).

[22] A. Manor and N. M. Shnerb, Journal of theoretical biology **253**, 838 (2008).

[23] O. Ovaskainen and B. Meerson, Trends in ecology & evolution **25**, 643 (2010).

[24] D. A. Kessler and N. M. Shnerb, Journal of Statistical Physics **127**, 861 (2007).

[25] D. A. Kessler and N. M. Shnerb, Journal of Physics A: Mathematical and Theoretical **41**, 292003 (2008).

[26] W. O. Kermack and A. G. McKendrick, Proceedings of the Royal society of London. Series A **138**, 55 (1932).

[27] D. A. Kessler and N. M. Shnerb, Physical Review E **76**, 010901 (2007).

[28] E. Moro, Physical Review E **70**, 045102 (2004).

[29] J. A. Bonachela, M. A. Muñoz, and S. A. Levin, Journal of Statistical Physics **148**, 723 (2012).

[30] S. D. Fuhlendorf, D. D. Briske, and F. E. Smeins, Applied Vegetation Science **4**, 177 (2001).

[31] K. Rasmussen, B. Fog, and J. E. Madsen, Global Environmental Change **11**, 271 (2001).

[32] T. J. Valone, M. Meyer, J. H. Brown, and R. M. Chew, Conservation Biology **16**, 995 (2002).

[33] J. Y. Zhang, Y. Wang, X. Zhao, G. Xie, and T. Zhang, New Zealand Journal of Agricultural Research **48**, 277 (2005).

[34] G. Allington and T. Valone, Journal of Arid Environments **74**, 973 (2010), ISSN 0140-1963, URL `http://www.sciencedirect.com/science/article/pii/S014019631`

[35] P. deMenocal, J. Ortiz, T. Guilderson, J. Adkins, M. Sarnthein, L. Baker, and M. Yarusinsky, Quaternary Science Reviews **19**, 347 (2000).

[36] J. Adkins, P. deMenocal, and G. Eshel, Paleoceanography **21**, PA1206 (2006).

[37] E. Ben-Jacob, H. Brand, G. Dee, L. Kramer, and J. Langer, Physica D: Nonlinear Phenomena **14**, 348 (1985).

[38] D. A. Kessler, Z. Ner, and L. M. Sander, Physical Review E **58**, 107 (1998).

[39] J. R. Tredicce, G.-L. Lippi, P. Mandel, B. Charasse, A. Chevalier, and B. Picque, American Journal of Physics **72**, 799 (2004).